Dendron-like Growth of Silver Nanoparticles Using a Water-Soluble Oligopeptide

Santanu Bhattacharya,[†] Apurba K. Das,[‡] Arindam Banerjee,*[,‡] and Dipankar Chakravorty*[,†]

Unit on Nano Science and Technology, Indian Association for the Cultivation of Science, Jadavpur, Kolkata 700032, India, and Department of Biological Chemistry, Indian Association for the Cultivation of Science, Jadavpur, Kolkata 700032, India

Received: January 24, 2006; In Final Form: April 21, 2006

A dendron-like nanostructure of silver was grown in solution using a water-soluble tetrapeptide Tyr-Aib-Tyr-Val (Aib, α-amino isobutyric acid), silver nitrate, and methanol. These structures are composed of silver nanoparticles having a bimodal size distribution with the median diameters around 2.0 and 19.5 nm, respectively. The dendron-like growth is ascribed to the effect of the local electric field generated by the dipoles associated with the peptide molecules. The optical absorption spectra have been analyzed by Mie scattering theory, which shows that there is a metal−nonmetal transition in silver particles having diameters less than ∼2.0 nm.

Introduction

Nanoparticles of noble metals have assumed importance in recent years because of their possible use in microelectronics and as catalysts.[1−4] Various templates have been used to encapsulate the desired materials into the channels or pores of the matrix,[5−10] some of the examples being carbon nanotubes, porous anodic alumina, polycarbonate membranes, and micelles. A challenging task in the synthesis of such materials is to develop methods to form superstructures using these nanoparticles. Some of the methods are the use of thiol-derivatized nanoparticles,[11] conventional lithographic processes,[12] LB techniques,[13] the use of DNA scaffolds,[14] and wet-chemical protocols using an aqueous surfactant solution.[15] In recent years silver and gold nanoparticles have been synthesized using alkylated tyrosine and amino acids.[16−19] We have adopted the strategy of using a water-soluble tetrapeptide Tyr-Aib-Tyr-Val (YUYV; Aib, α-amino isobutyric acid) solution for reducing silver ions in $AgNO_3$ solution to metallic silver. We observed a dendron-like structure formed by nanoparticles of silver. Silver particle sizes were found to be bimodal giving rise to two absorption peaks. The analysis of the data led to the conclusion of a metal−nonmetal transition in silver particles with diameters less than ∼2 nm. The details are presented in this paper.

Experimental Section

The chemicals used for the present synthesis were the tetrapeptide, silver nitrate, and methanol. The tetrapeptide was prepared by conventional solution-phase methodology.[20] In a typical run, the steps were as follows: 8 mL of tetrapeptide solution (7.5 mmol) in methanol was added to 8 mL of Milli-Q water, 17 mg of $AgNO_3$ (5 mmol) was dissolved in 20 mL of methanol−Milli-Q water (1:1) solution. Then, 12 mL of the peptide solution was added to 60 mL of $AgNO_3$ solution under vigorous stirring in a dark chamber. The pH of the latter mixture was adjusted to a value of ∼8 with standard NaOH solution.

* Authors to whom correspondence should be addressed. Fax: (+91) 33 2473-2805. E-mail: bcab@mahendra.iacs.res.in (A.B.); mlsdc@mahendra.iacs.res.in (D.C.).

[†] Unit on Nano Science and Technology.

[‡] Department of Biological Chemistry.

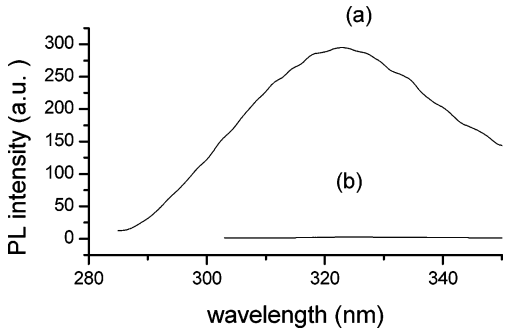

Figure 1. Fluorescence spectra of the peptide solution at different stages of the reaction: (a) peptide solution (original); (b) after formation of silver nanoparticles

The color of the transparent solution changed from light yellow to strong yellow under stirring for 4 h, which indicated the formation of colloidal silver particles via the oxidation of the tyrosine residues of the tetrapeptide. The evidence for the oxidation of the tyrosine residues is provided by the fluorescence spectrum of the above solution at ∼300 nm as shown in Figure 1. It is evident that the fluorescence is drastically diminished for the solution confirming the primary role of tyrosine in the reduction process of silver ions.

The microstructure of the silver particles was investigated by a JEOL 2010 transmission electron microscope. For microscopy a few drops of the peptide solution containing the nanoparticles were placed on carbon-coated grids. After the solution evaporated the grid was mounted in the specimen chamber of the microscope. Optical absorption spectra of the silver particles dispersed in methanol were recorded with a UV-1601 PC UV−vis scanning spectrometer.

Results and Discussion

Figure 2a is a transmission electron micrograph showing the formation of dendron-like structures. Figure 2b is a micrograph taken at higher magnification indicating the formation ofa dendron-like structure by interconnection of nanoparticles. For delineation of the particle size distribution we consider the micrographs shown in Figures 3a and 3b, which are electron

10.1021/jp0604847 CCC: $33.50
Published on Web 05/17/2006

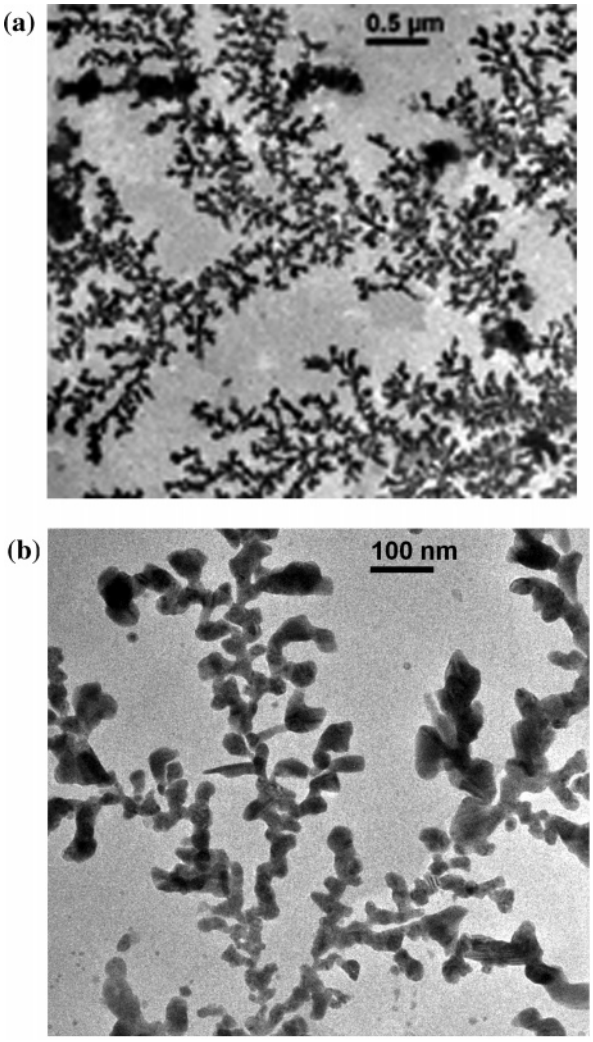

Figure 2. Transmission electron micrograph of dendron-like silver nanostructures grown using tetrapeptide at different magnifications: (a) scale bar = 0.5 μm; (b) scale bar = 100 nm.

micrographs taken at a higher magnification than that used for Figures 2a and 2b. Figure 4 is the electron diffraction pattern obtained from Figure 3. The pattern was taken with an electron beam with a diameter of 15 nm. The interplanar spacings calculated from the diffraction data are summarized in Table 1 and compared with American Society for Testing and Materials (ASTM) data. These confirm that the dendron-like structures consist of metallic silver only. Figure 5 is a high-resolution electron micrograph taken from one of the silver nanoparticles. The lattice planes are clearly visible, and the interplanar spacing is estimated to be 0.2 nm, which again confirms the presence of metallic silver in these particles. The particle size distribution obtained from Figure 3 is shown in Figure 6. Clearly, it can be visualized that there is a bimodal distribution. These data were fitted to a log-normal distribution function,[21] and the extracted values of the median diameter and the geometric standard deviation are $\overline{d_1} = 2.0$ nm, $\sigma_1 = 1.7$, and $\overline{d_2} = 19.5$ nm, $\sigma_2 = 1.4$, respectively. The geometric standard deviation σ has been defined as

$$\ln \sigma = \left[\left\{\sum_i n_i(\ln x_i - \ln \bar{x})^2 / \sum_i n_i\right\}\right]^{1/2} \qquad (1)$$

The lines are the theoretical fits, and the points represent the experimental data in Figure 6.

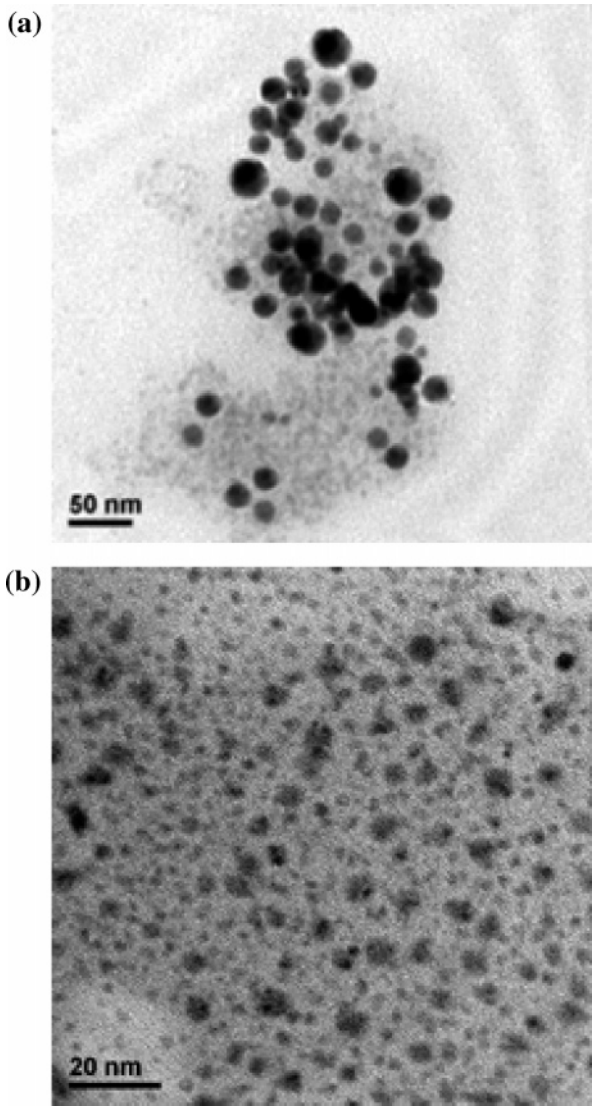

Figure 3. Transmission electron micrograph of Figure 1 at different magnifications: (a) scale bar = 50 nm; (b) scale bar = 20 nm

TABLE 1: Comparison of Interplanar Spacings d_{hkl} Obtained from the Specimen Electron Diffraction Pattern with ASTM Values

observed d_{hkl} (nm)	ASTM[34] silver (nm)
0.2405	0.2425
0.2256	0.2236
0.1977	0.2000
0.1412	0.1443
0.1216	0.1212
0.1184	0.1170
0.10704	0.1118
0.09817	0.1000

Figure 7 shows the variation of the optical absorption coefficient as a function of wavelength for silver nanoparticles. There are two absorption peaks present, one around 340 nm and the other around 450 nm. The two peaks are explained to arise due to the two sets of silver nanoparticles present in the system; e.g., the peak at 340 nm is ascribed to those with median diameters of 2.0 nm, and the one at 450 nm is believed to arise due to particles with a median diameter of 19.5 nm. This is further discussed subsequently.

The dendron-like growth of metallic silver is rather interesting. Such growth processes were extensively studied earlier in the case of electrodeposited metals.[22−26] The dendritic growth

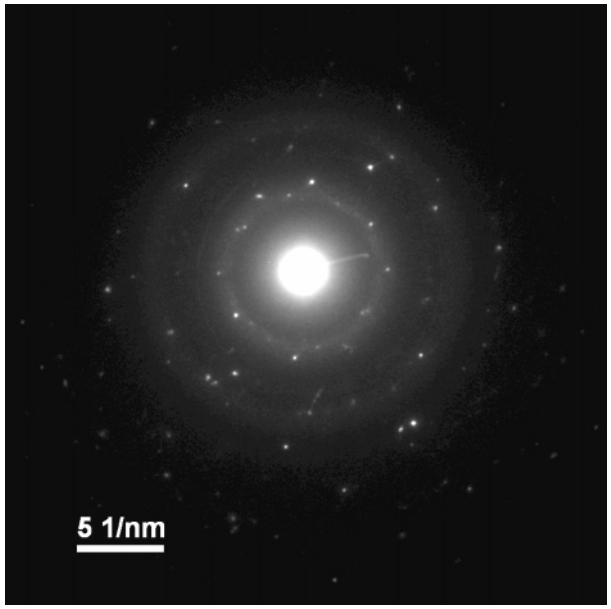

Figure 4. Electron diffraction pattern obtained from Figure 3.

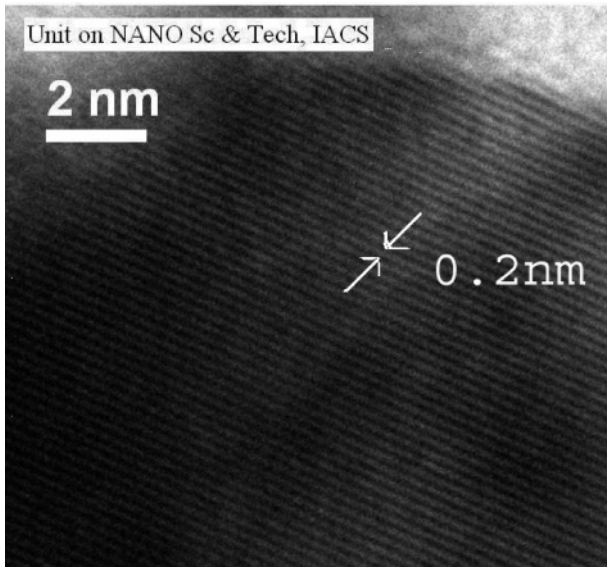

Figure 5. High-resolution electron micrograph of one silver nanoparticle.

was explained as arising due to a diffusion-limited growth process. A random walk mechanism was invoked. In the present system, no external electric field was applied. However, the peptide molecules possess dipole moments of their own.[27,28] This means that the peptide molecules in the bath solution make up a system of randomly aligned dipoles. These molecules not only provide the nucleation sites for the growth of silver nanoparticles but also produce electric fields in their vicinities. Silver ions therefore carry out a random walk process under the influence of such an electric field near each molecule and produce dendritic growth.

The bimodal distribution of the silver particle sizes can be rationalized as follows. The nature of the chemical process involved in the present system indicates that the peptide molecules act as heterogeneous nucleation sites for the growth of silver particles. Initially, particles of an average diameter of 2 nm are formed. As the reaction is allowed to proceed these particles start becoming aggregated producing larger particles. There is however a saturation limit to the diameter of these particles set by the dimension of the interconnected peptide

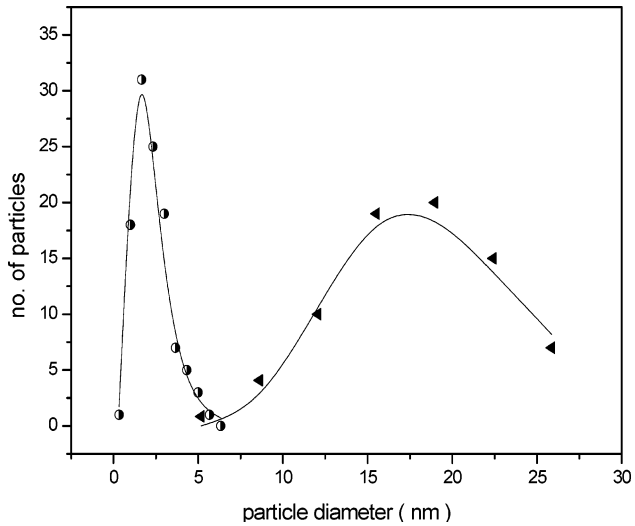

Figure 6. Particle size distribution obtained from Figure 3.

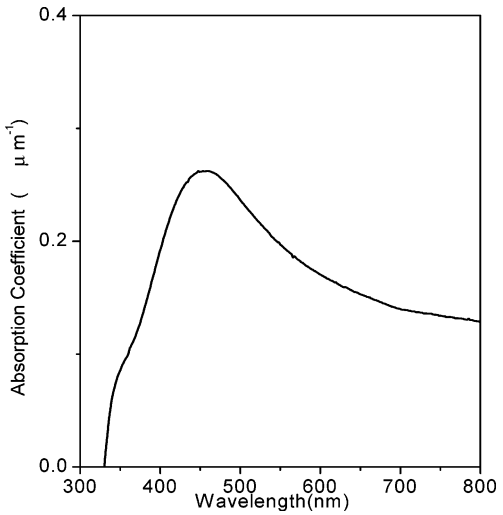

Figure 7. Variation of the optical absorption coefficient as a function of wavelength for silver nanoparticles dispersed in a liquid medium.

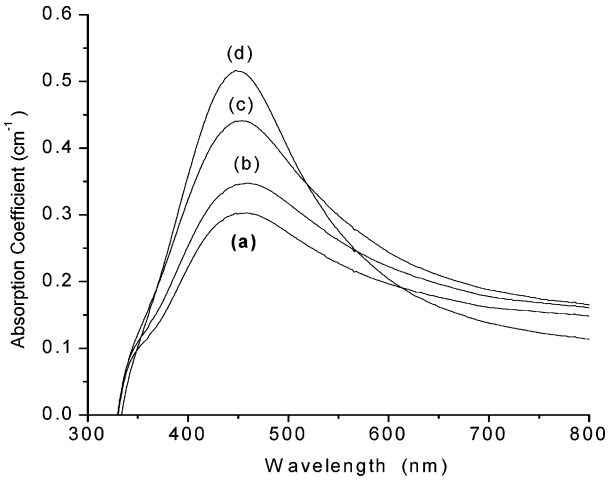

Figure 8. Optical absorption spectra for silver particles synthesized for different periods of reaction: (a) 4 h; (b) 5.5 h; (c) 7 h; (d) 8.5 h.

molecular aggregates.[29] This can be seen from the change of the optical absorption spectrum as a function of reaction time as shown in Figure 8. In this figure it can be seen that as the reaction time increases from 4 to 8.5 h the absorption peak around 450 nm increases in magnitude and that around 340 nm gradually disappears.

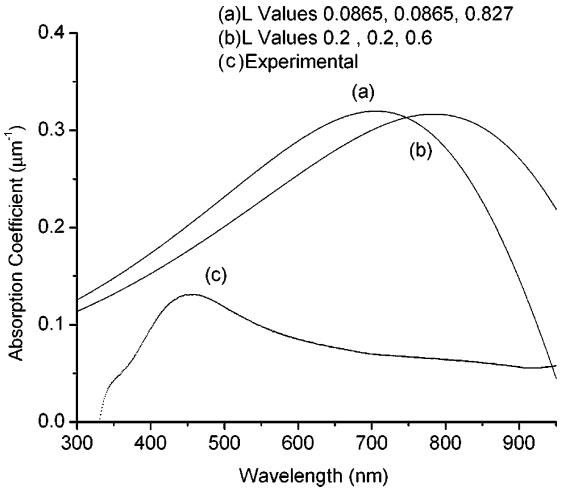

Figure 9. Analysis of the optical absorption spectra using (a) Maxwell−Garnett effective medium theory or (b) dipole−dipole coupling between neighboring particles. (c) Experimental results.

It must be mentioned here that the larger structures as depicted by the dendron-like configuration are in fact a reflection of the arrangement of the nanosized metal particles in a particular way. The latter has been adduced to a diffusion-limited random walk process. The analysis of optical absorption spectra will be discussed on the basis of both Mie scattering theory as well as Maxwell−Garnett effective medium approximation. The former is applicable for the case in which the volume fraction of the dispersed metal particles is small, and the latter is invoked when there is a possibility of interaction between particles in determining optical absorption. It will be seen that the model of dipole−dipole interaction between metal particles fails to predict the observed experimental data. Also, we explore the possibility of the particles not being spherical in shape.

We first consider the Maxwell−Garnett effective medium theory in which dipole−dipole coupling between adjacent particles has been taken into account. According to this model the effective dielectric permittivity $\bar{\epsilon}$ is written as[30]

$$\bar{\epsilon} = \epsilon_m \frac{1 + 2/3f\alpha'}{1 - 1/3f\alpha'} \tag{2}$$

where ϵ_m is the dielectric permittivity of the medium in which the particles are dispersed, f is the volume fraction of the particles, and α' is given by

$$\alpha' = \frac{1}{3}\sum_{j=1}^{3} \frac{\epsilon_p - \bar{\epsilon}}{\epsilon + L_j(\epsilon_p - \bar{\epsilon})} \tag{3}$$

where the L_j values are the triplets of the depolarization factors. For spherical particles, $L_1 = L_2 = L_3 = {}^1/_3$.

We have tried to fit the experimental optical absorption data to eqs 2 and 3 in a self-consistent manner. Assuming ellipsoidal shapes of the particles, we introduced values of $L_1 = 0.0865$, $L_2 = 0.0865$, and $L_3 = 0.827$.[30] The theoretical curves are as shown in Figure 9. These predict an absorption maximum at a different wavelength altogether as compared to that of the experimental data. Next, the dipole−dipole coupling between neighboring particles was taken into account by using effective depolarization factors L_j*, which replaced the L_j values in eq 3.[30] We have taken the values L_1* = 0.2, L_2* = 0.2, and L_3* = 0.6. The theoretical curves are shown in Figure 9. Again they are at variance with the experimental data. We therefore conclude that the particles are not ellipsoidal nor is there any dipole−dipole coupling between neighboring particles.

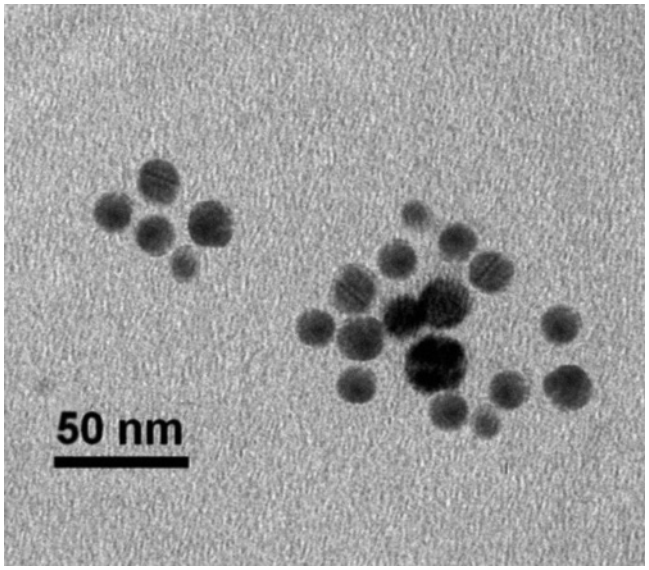

Figure 10. Transmission electron micrograph that shows individual particles are spherical.

Examining the electron micrographs carefully we conclude that the particles form a dendron-like structure, but the volume fraction is sufficiently low to preclude the possibility of any nearest-neighbor interaction between the particles. Also the silver particles are essentially spherical in shape. Any apparent nonsphericity arises because of the superposition of particles at different planes of the electron microscope specimen. In Figure 10 we show a transmission electron micrograph for a specimen prepared after only 2 h of reaction time. It can be seen that the particles are spherical.

In view of the above discussion we have analyzed the optical absorption data by Mie scattering theory, which gives the absorption coefficient α as follows

$$\alpha \equiv \sum_j \frac{18\pi f_j \epsilon_m^{3/2} \epsilon 2j}{\lambda[(\epsilon_{1j} + 2\epsilon_m)^2 + \epsilon_{2j}^2]} \tag{4}$$

where $\times a6_j$ is the volume fraction of particles with diameter d_j, ϵ_m is the dielectric constant of the medium (here methanol) in which the nanoparticles are dispersed, and ϵ_j ($= \epsilon_{1j} + i\epsilon_{2j}$) is the dielectric constant of the metal phase with diameter d_j. The size-dependent dielectric constant for a metal particle is given by[31]

$$\epsilon_j = \left(1 - \frac{\omega_p^2}{\omega^2}\right) + i\left[\frac{\omega_p^2}{\omega^3}\left(\frac{\sigma_j}{\epsilon_0} + \frac{^2V_f}{d_j}\right)\right] \tag{5}$$

where ω_p is the plasmon frequency, ω the angular frequency, σ_j the direct current conductivity of a particle with diameter d_j, ϵ_0 the free space permittivity, and V_f the Fermi velocity of the bulk metal. The experimental absorption coefficient data were least-squares-fitted to eqs 4 and 5 using σ_j, $\times a6$, and ϵ_m as parameters. The value of V_f for silver was taken as 1.4×10^{15} nm/s and that of ω_p as 1.4×10^{16} rad/s.[32] In Figure 11 curves a and b represent the theoretical fits, and curve c corresponds to the experimental data. The values of f and ϵ_m were extracted to be 2.1×10^{-3} and 6.4, respectively. These are consistent with the microstructure and the dielectric medium used for measurement. The conductivity values for different particle

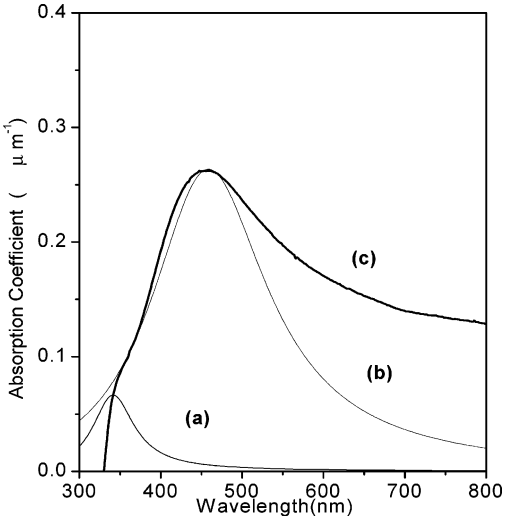

Figure 11. Optical absorption data fitting by Mie's theory: (a and b) theoretical curves; (c) experimental curve.

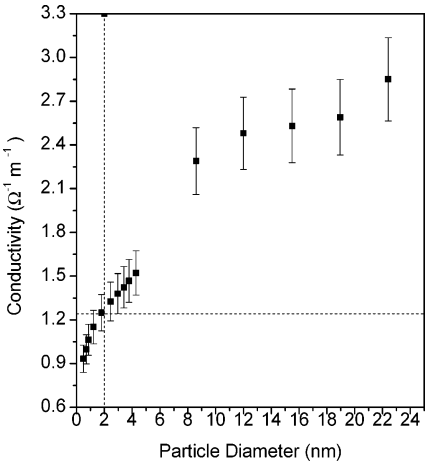

Figure 12. Extracted values of electrical conductivity as a function of silver particle diameter.

diameters as extracted by the least-squares-fitting are summarized in Figure 12. It is interesting to note that below a particle size of ~2.0 nm the conductivities have values below Mott's minimum metallic conductivity σ_m as given by the expression[33]

$$\sigma_m \cong \frac{0.06e^2}{\hbar a}\left(\frac{6}{z}\right)^2 \quad (6)$$

where $\hbar$ is Planck's constant, e is the electronic charge, a the interatomic distance, and z the coordination number. For the case of silver, this value turns out to be 1.2×10^4 ohm^{-1} m^{-1}. We therefore conclude that for particle diameters smaller than 2.0 nm there is a metal−nonmetal transition for silver.

Conclusions

In conclusion, we have successfully utilized a tetrapeptide to reduce silver ions and also to generate dendron-like silver nanostructures composed of silver nanoparticles. The particle size shows a bimodal distribution. The dendron-like structure is ascribed to the silver growth under the influence of the local electric field generated by the dipoles inherent in the peptide molecules. Optical absorption measurements have been carried out that show two peaks, one around 340 nm and the other one at around 450 nm. Analysis by effective medium theory shows that the particles do not have dipole−dipole interactions among them. From the analysis of the data by Mie's scattering theory it is concluded that there is a metal−nonmetal transition for particles having diameters less than ~2.0 nm.

Acknowledgment. S.B. thanks the CSIR, New Delhi, for the award of a Junior Research Fellowship. A.K.D. thanks the CSIR for the award of a Senior Research Fellowship. D.C. thanks the Indian National Science Academy, New Delhi, for the award of a Senior Scientist position. The work was carried out under the Nano Science and Technology Initiative of the Department of Science and Technology, Government of India, New Delhi.

References and Notes

(1) Andres, R. P.; Bielefeld, J. D.; Henderson, J. I.; Janes, D. B.; Kolagunta, V. R.; Kubiak, C. P.; Mahoney, W. J.; Osifchin, R. G. *Science* **1996**, *273*, 1690.
(2) Förster, S.; Antonietti, M. *Adv. Mater.* **1998**, *10*, 195.
(3) Zhou, Y.; Yu, S. H.; Wang, C. Y.; Li, X. G.; Zhu, Y. R., Chen, Z. Y. *Adv. Mater.* **1999**, *11*, 850.
(4) Zhu, J.; Liao, X.; Chen, H. Y. *Mater. Res. Bull.* **2001**, *36*, 1687.
(5) Zhachuk, R. A.; Tils, S. A.; Olshanetskl, B. Z. *JETP Lett.* **2004**, *79*, 381.
(6) Martin, C. R. *Chem. Mater.* **1996**, *8*, 1739.
(7) Sapp, S. A.; Lakshmi, B. B.; Martin, C. R. *Adv. Mater.* **1999**, *11*, 402.
(8) Dai, H.; Wong, E. W.; Lu, Y. Z.; Fan. S.; Lieber, C. M. *Nature* **1995**, *375*, 769.
(9) Zhang, Z.; Ying. J. Y.; Dresselhans, M. S. *J. Mater. Res.* **1998**, *13*, 1745.
(10) Martin, C. R. *Science* **1994**, *266*, 1961.
(11) Schöllhorn, R. *Chem. Mater.* **1996**, *8*, 1747.
(12) Sarathy, K. V.; Kulkarni, G. U.; Rao, C. N. R. *Chem. Commun.* **1997**, 537.
(13) Thalladi, V. R.; Whitesides, G. M. *J. Am. Chem. Soc.* **2002**, *124*, 3520.
(14) Yang, P. *Nature* **2003**, *425*, 243.
(15) Warner, M. G.; Hutchison, J. E. *Nat. Mater.* **2003**, *2*, 272.
(16) Doty, R. C.; Tshikhudo, T. R.; Brust, M.; Ferrig, D. G. *Chem. Mater.* **2005**, *17*, 4630.
(17) Bjerneld, E. J.; Johansson, P.; Kall, M. *Single Mol.* **2000**, *1*, 239.
(18) Bhargava, S. K.; Booth, J. M.; Agrawal, S.; Coloe, P.; Kar, G. *Langmuir* **2005**, *21*, 5949.
(19) Swami, A.; Kumar, A.; D'costa, M.; Pasricha, R.; Sastry, M. *J. Mater. Chem.* **2004**, *14*, 2696.
(20) Bodanszky, M.; Bodanszky, A. *The Practice of Peptide Synthesis*; Springer-Verlag: New York, 1984; pp 1−282.
(21) Roy, B.; Chakravorty, D. *J. Phys.: Condens Matter* **1990**, *2*, 9323.
(22) Brady, R. M.; Ball, R. C. *Nature* **1984**, *309*, 225.
(23) Argoul, F.; Arnedo, A.; Gassean, G.; Swinney, H. L. *Phys Rev. Lett.* **1988**, *61*, 2558.
(24) Hibbert, D. B.; Melrose, J. R. *Proc. R. Soc. London, Ser. A* **1989**, *423*, 149.
(25) Matsushita, M.; Sano, M.; Hayakawa, Y.; Honjo, H.; Sawada, Y. *Phys. Lett.* **1989**, *53*, 286.
(26) Roy, S.; Chakravorty, D. *Phys. Rev. B* **1993**, *47*, 3089.
(27) Tartaglia, G. G.; Cavalli, A.; Pellarin, R.; Caflisch, A. *Protein Sci.* **2004**, *13*, 1939.
(28) Antoine, R.; Compagnon, I.; Rayane, D.; Broyer, M.; Dugourd, P.; Breaux, G.; Hagemeister, F. C.; Pippen, D.; Hudgins, R. R.; Jarrold, M. F. *Eur. Phys. J. D* **2002**, *20*, 583.
(29) Das, A. K.; Haldar, D.; Hegde, R. P.; Shamala, N.; Banerjee, A. *Chem. Commun.* **2005**, 1836.
(30) Granqvist, C. G.; Hunderi, O. *Phys. Rev. B* **1978**, *18*, 2897.
(31) Kreibig, U. *J. Phys. F: Met. Phys.* **1974**, *4*, 999.
(32) Kittel, C. *Introduction to Solid State Physics*; Wiley: New York, 1961; p 374.
(33) Mott, N. F.; Davis, E. A. *Electron Processes in Non-Crystalline Materials*; Clarendon Press: Oxford, U. K., 1971; p 26.
(34) Novgorodova, D.; Gorshkov, A.; Mokhov, A. *Zap. Vseross. Mineral. O-va.* **1979**, *108*, 552.